Vapor–Liquid Equilibrium of Pure Fluids from a Simple Thermodynamic Perturbation Theory

S. Lago,* J. L. Lopez-Martín, B. Garzón, and C. Vega

Departamento Química Física I, Facultad CC Químicas, Universidad Complutense, E-28040 Madrid, Spain

Received: August 2, 1993; In Final Form: February 22, 1994®

We derive a perturbation theory for linear and nonlinear molecules interacting through the Kihara potential. This theory may be considered as a simplified version of more elaborated treatments previously proposed for this model. An advantage of the new formulation is that expressions for Helmholtz free energy, pressure, and entropy are analytical so that vapor–liquid determination becomes an easy task. Vapor–liquid equilibria obtained from the theory showed fair agreement with simulation results of the model. Moreover, we compared theoretical predictions of coexistence densities and vapor pressures with experimental results for ethane, carbon dioxide, and benzene. Good agreement was found in all the cases over a broad range of temperatures. The presented treatment combines the simplicity required in chemical engineering applications with well-defined approximations on a statistical thermodynamic treatment.

I. Introduction

An important problem in chemical engineering is the determination of phase diagram of complex fluid mixtures.[1] A first step toward the solution to this problem is the previous determination of the vapor–liquid equilibrium curve (VLE) of pure components of the mixture. This curve is obtained by imposing equality of temperature, pressure, and chemical potential in both phases. For industrial purposes, virial equation truncated after the second term for the vapor phase and an empirical equation of state (EOS) for the liquid phase are commonly used. These EOS usually have a simple form, cubic or slightly more complicated, and contain many empirical parameters whose physical meaning is sometimes obscure. Furthermore, these parameters are functions of density and/or temperature. However, these equations of state, which usually take the name of their first proposers (Redlich–Kwong,[2] Peng–Robinson,[3] Deiters,[4] etc.) are quite useful because they allow an easy determination of pressures at coexistence and densities of important fluids within a few hundredths of error.[5]

The point of view of a physical chemist, however, is focused on the determination of the pair correlation function (PCF). This function is obtained either from simulation or by solving some involved integral equation. Then by using an exact relation (virial, compressibility) or a thermodynamic perturbation theory, it is possible to obtain thermodynamic properties at any point so that phase equilibria may be determined. This straightforward way involves such high temporal costs in terms of computer or personal time that it becomes unacceptable for industry. We think however that with little effort, some present results from molecular-based theories can be applied to solve relevant industrial problems such as VLE. The main goal of this paper is to show how it is possible to build a useful link between liquid-state statistical mechanics and practical problems.

The theoretical tool chosen in this paper is the thermodynamic perturbation theory (TPT). This kind of theory is based on an appropriate splitting of microscopic attractive and repulsive intermolecular forces. It has been applied in a rigorous way to important liquids,[6] and excellent results were obtained. Hereafter, we refer to this rigorous version of perturbation theory as RPT. The theory however is too involved, and we present here an alternative treatment based on previous work of one of us.[7] This alternative will be called hereafter simple perturbation theory (SPT). The SPT is based on a semiempirical approach to PCF. This approach was obtained from simulation and is directly linked to molecular shape and size. Thus, Lago and Boublík[7] were able to obtain good results for binary mixtures but only for $p = 0$. In this paper, we present results at any pressure, and therefore we are able to solve the equilibrium equations. So, the scheme of this paper is as follows: section II is devoted to a brief review of the old version of SPT, introducing the molecular model, and showing how the equations for pressure and chemical potential can be derived so that VLE may be computed. Section III shows the comparison between the results obtained here, the RPT, and Monte Carlo simulations for modeled liquids. Section IV shows the application to some important real liquids and illustrates how the observed systematic deviations can be corrected to give good results for VLE. Finally, section V contains a short discussion of the results including new values for the vaporization enthalpy. The possibility to apply the theory presented here to more complex systems is also considered in section V.

II. Molecular Model and Theory

In the model presented here, first proposed by Kihara,[8] molecules are represented by a linear segment of length L. The value of L is close to the length of the chemical bond. "Bonds" of different molecules interact through a Lennard-Jones-like potential:

$$u(\rho) = 4\epsilon\left[\left(\frac{\sigma}{\rho(r_{12},\omega_1,\omega_2)}\right)^{12} - \left(\frac{\sigma}{\rho(r_{12},\omega_1,\omega_2)}\right)^{6}\right] \quad (1)$$

but $\rho = \rho(r_{12},\omega_1,\omega_2)$ means here the distance between these bonds and depends on the distance between centers of mass r_{12} as well as on molecular orientations ω_1,ω_2 with respect to the vector joining the centers of mass. ϵ and σ are two parameters with dimensions of energy and length, respectively, characterizing the intermolecular interaction. Molecular elongation or reduced length is defined as $L^* = L/\sigma$. Previous experience[6,7] shows that only one bond adequately represents true linear molecules and others which are not strictly linear but have a linear carbonated skeleton as in ethane or ethylene. An extensive simulation has been carried out for linear models in the Gibbs ensemble.[9] So, the VLE curve has been determined for different molecular elongations in practically all the liquid range. Moreover, a rigorous perturbation theory (RPT) has been presented.[13] In this theory, PCF is obtained by solving the RHNC integral equation.[10,11] Excellent agreement with simulation[12] and experiment[6] has been obtained in this way. We have developed algorithms where the entire procedure of solving RHNC, obtaining thermodynamic properties and finally solving equilibrium equations takes only a few seconds using a PC. However, the method still remains time consuming and complicated for the industry, and hence the simplified version of this theory SPT is presented in this section.

® Abstract published in *Advance ACS Abstracts*, April 1, 1994.

0022-3654/94/2098-5355$04.50/0

Nonlinear molecules can be modeled by a set of bonds defining a geometrical body mimicking the shape of the molecule.[13] This geometrical body is called the molecular core. The relevant geometrical quantities are the volume, V^C, the surface area, S^C and $^1/_{4\pi}$ times the mean curvature, R^C of core.[14] Reduced variables are used as necessary and are defined as $T^* = kT/\epsilon$ and $p^* = p\sigma^3/\epsilon$.

Only numerical results for pure substances are presented in this paper. However we shall present the general formalism for a multicomponent mixture. The generalization of eq 1 to a multicomponent mixture is given by

$$u^{\gamma\lambda}(\rho^{\gamma\lambda}) = 4\epsilon_{\gamma\lambda}\left[\left(\frac{\sigma^{\gamma\lambda}}{\rho^{\gamma\lambda}(r_{12},\omega_1,\omega_2)}\right)^{12} - \left(\frac{\sigma^{\gamma\lambda}}{\rho^{\gamma\lambda}(r_{12},\omega_1,\omega_2)}\right)^{6}\right] \quad (2)$$

Thus, all our formulas will be given for a multicomponent mixture without loss of generality.

The essential step in TPT is the splitting of total potential into two parts, the reference potential, u_0, whose properties are well-known and the perturbation potential, u_1. In the Weeks–Chandler–Andersen (WCA) version[15] of TPT the potential is divided into a term involving repulsive forces u_0 and another u_1 containing the attractive ones. For a Kihara potential u_0 and u_1 are written as

$$u_0^{\gamma\lambda}(\rho^{\gamma\lambda}) = u^{\gamma\lambda}(\rho^{\gamma\lambda}) + \epsilon_{\gamma\lambda} \qquad \rho^{\gamma\lambda} < q_{\gamma\lambda} \quad (3)$$

$$u_0^{\gamma\lambda}(\rho^{\gamma\lambda}) = 0 \qquad \rho^{\gamma\lambda} > q_{\gamma\lambda} \quad (4)$$

$$u_1^{\gamma\lambda}(\rho^{\gamma\lambda}) = -\epsilon^{\gamma\lambda} \qquad \rho^{\gamma\lambda} < q_{\gamma\lambda} \quad (5)$$

$$u_1^{\gamma\lambda}(\rho^{\gamma\lambda}) = u^{\gamma\lambda}(\rho^{\gamma\lambda}) \qquad \rho^{\gamma\lambda} > q_{\gamma\lambda} \quad (6)$$

where $q_{\gamma\lambda} = 2^{1/6}\sigma^{\gamma\lambda}$.

Expansion of the Helmholtz free energy A about the reference system truncated at the first perturbation term yields

$$\frac{A - A^*}{NkT} = \frac{A^\circ - A^*}{NkT} + \frac{n}{2kT}\sum_{\lambda,\gamma} x_\gamma x_\lambda \int u_1^{\gamma\lambda}(\rho^{\gamma\lambda})\, g^\circ_{\gamma\lambda}(\rho^{\gamma\lambda})\, S_{\gamma+\rho+\lambda}\, d\rho \quad (7)$$

Here A° and A^* are the Helmholtz free energies of reference system and of an ideal gas, respectively; n is the number density and x_α is the mole fraction of component α. $g^\circ_{\gamma\lambda}(\rho^{\gamma\lambda})$ is the PCF of the reference system, and $S_{\gamma+\rho+\lambda}$ is the mean surface of the body formed when a molecule λ moves around a molecule γ keeping constant their shortest distance $\rho^{\gamma\lambda}$. $S_{\gamma+\rho+\lambda}$ can be related to the surfaces and to the $^1/_{4\pi}$ times the mean curvature of individual molecules by[14]

$$S_{\gamma+\rho+\lambda} = S_\gamma + S_\lambda + 8\pi(R_\gamma + R_\lambda)\rho + 4\pi\rho^2 \quad (8)$$

We denote $S_{\gamma+0+\lambda}$ simply as $S_{\gamma+\lambda}$ or $S_{\gamma\lambda}$ unless confusion arises. The second term in the right-hand side of eq 7 is usually known as the first perturbation term and denoted as A_1.

The next step is to relate the Helmholtz free energy and PCF of the reference system to that of hard convex bodies, the so-called representative bodies. A new expansion of A_0 gives as final expression[7]

$$\frac{A - A^*}{NkT} = \frac{A^{hcb} - A^*}{NkT} + \frac{n}{2kT}\sum x_\gamma x_\lambda \int u_1^{\gamma\lambda}(\rho^{\gamma\lambda})\, g^{hcb}_{\gamma\lambda}(\rho^{\gamma\lambda})\, S_{\gamma+\rho+\lambda} d\rho^{\gamma\lambda} - n x_\gamma x_\lambda g^{hcb}_{\gamma\lambda}(0)\, S_{\gamma+d+\lambda}\{d_{\gamma\lambda} - \int_0^{q_{\gamma\lambda}}(1 - \exp[-u_0^{\gamma\lambda}/kT])\, d\rho\} \quad (9)$$

where

$$d_{\lambda\lambda} = \int_0^{q_{\lambda\lambda}}(1 - \exp[-u_0^{\lambda\lambda}/kT])\, d\rho \quad (10)$$

$$d_{\gamma\lambda} = (d_{\gamma\gamma} + d_{\lambda\lambda})/2 \quad (11)$$

Superscript hcb refers to the properties of representative hard convex bodies (HCB) in the above equations. $d_{\lambda\lambda}$ defines the thickness of these HCBs and represents an extension of hard-sphere diameter as defined in the Barker–Henderson TPT.[16] HCB is built as the parallel body to the molecular core at the distance $d_{\lambda\lambda}/2$. Its volume, surface area, and $^1/_{4\pi}$ times mean curvature are denoted respectively by V_λ, S_λ, and R_λ.

In our previous paper[7] the total correlation function, $h = g - 1$, was approximated as

$$h_{\gamma\lambda}(\rho^{\gamma\lambda}) = A_{\gamma\lambda} + B_{\gamma\lambda}\frac{S_{\gamma\lambda} + 4\pi\rho R_{\gamma\lambda}}{S_{\gamma+\rho+\lambda}} \qquad 0 < \rho^{\gamma\lambda} < b_{\gamma\lambda} \quad (12)$$

$$h_{\gamma\lambda}(\rho^{\gamma\lambda}) = 0 \qquad \rho^{\gamma\lambda} > b_{\gamma\lambda} \quad (13)$$

where $A_{\gamma\lambda}$, $B_{\gamma\lambda}$, and $b_{\gamma\lambda}$ are defined by

$$A_{\gamma\lambda} = [1 - g^{hcb}_{\gamma\lambda}(0)]\frac{S_{\gamma\lambda} + 4\pi R_{\gamma\lambda} b_{\gamma\lambda}}{4\pi R_{\gamma\lambda} b_{\gamma\lambda} + 4\pi b_{\gamma\lambda}^2} \quad (14)$$

$$B_{\gamma\lambda} = [g^{hcb}_{\gamma\lambda}(0) - 1]\frac{S_{\gamma\lambda} + 8\pi R_{\gamma\lambda} b_{\gamma\lambda} + 4\pi b_{\gamma\lambda}^2}{4\pi R_{\gamma\lambda} b_{\gamma\lambda} + 4\pi b_{\gamma\lambda}^2} \quad (15)$$

$$b_{\gamma\lambda} = R_{\gamma\lambda}/g^{hcb}_{\gamma\lambda}(0) \quad (16)$$

and $R_{\gamma\lambda} = R_\gamma + R_\lambda$.

In eqs 14–16, $g^{hcb}_{\gamma\lambda}(0)$ is the contact PCF, which can be expressed approximately as[7]

$$g^{hcb}_{\gamma\lambda}(0) = \frac{1}{(1-v)} + \frac{S_\gamma S_\lambda (r-t) + (S_\gamma T_\lambda - T_\gamma S_\lambda)s}{(1-v)^2 S_{\gamma+\lambda}} + \frac{2 S_\gamma S_\lambda q s}{9(1-v)^3 S_{\gamma+\lambda}} \quad (17)$$

The lower case letters are related to the properties of representative hard convex bodies by the general expression

$$y = n\sum_\lambda x_\lambda Y_\lambda \quad (18)$$

where Y_λ denotes any geometrical property of HCB α. Furthermore

$$Q_\lambda = R_\lambda^2 \quad (19)$$

$$T_\lambda = 4\pi R_\lambda^3/S_\lambda \quad (20)$$

Considering eqs 14–20 and with the definitions

$$\delta_{\gamma\lambda} = d_{\gamma\lambda}/q_{\gamma\lambda} \quad (21)$$

$$\Delta_{\gamma\lambda} = (d_{\gamma\lambda} + b_{\gamma\lambda})/q_{\gamma\lambda} \quad (22)$$

we finally obtain for the Helmholtz free energy:[7]

$$\frac{A-A^*}{NkT}=\frac{A^{hcb}-A^*}{NkT}+\frac{n}{2kT}\sum_{\gamma,\lambda}x_\gamma x_\lambda q_{\gamma\lambda}\epsilon_{\gamma\lambda}\left\{(\alpha_{\gamma\lambda}-p_{\gamma\lambda})\left(\frac{2\Delta_{\gamma\lambda}^{-3}}{3}-\frac{\Delta_{\gamma\lambda}^{-9}}{9}\right)+(\beta_{\gamma\lambda}-n_{\gamma\lambda})\left(\frac{\Delta_{\gamma\lambda}^{-4}}{2}-\frac{\Delta_{\gamma\lambda}^{-10}}{10}\right)+(\omega_{\gamma\lambda}-m_{\gamma\lambda})\left(\frac{2\Delta_{\gamma\lambda}^{-5}}{5}-\frac{\Delta_{\gamma\lambda}^{-11}}{11}\right)+\frac{\alpha_{\gamma\lambda}}{3}\left(\delta_{\gamma\lambda}^{3}-\frac{8}{3}\right)+\frac{\beta_{\gamma\lambda}}{2}\left(\delta_{\gamma\lambda}^{2}-\frac{9}{5}\right)+\omega_{\gamma\lambda}\left(\delta_{\gamma\lambda}-\frac{72}{55}\right)-M\right\} \quad (23)$$

where all the symbols in the eq 23 are related in analytic form to molecular properties and the explicit expressions are given in ref 7 and can also be found in appendix A. Strictly speaking, eq 23 can be applied only if $\Delta > 1$, but this is the most usual case, and we have not observed any exception with physical meaning to this rule.

Equation 23 was applied to obtain excess properties of relatively complex mixtures of molecules irrespective of their shape. Results agreed well enough with experiment, but their scope was limited by the lack of simulation results and by the fact that computations were made also at zero pressure. It is possible to obtain derivatives of Helmholtz free energy and get explicit expressions for pressure and entropy. However, this task is cumbersome. Therefore we used a computer program of symbolic computation including automatic translation to FORTRAN language to avoid error. In this way we were able to obtain analytical expressions for pressure and consequently for chemical potential and, thus, to calculate the VLE curve.

Explicitly, equations allowing the calculation of the pressure are given by

$$P=-(\partial A/\partial V)_T \quad (24)$$

$$P=P_0+P_1 \quad (25)$$

Here P_0 and P_1 are respectively the pressure terms coming from reference and perturbation Helmholtz free energy. P_0 corresponds to the EOS already given by Boublík:

$$\frac{P_0}{nkT}=\frac{9nv(v-1)^2-s[qs(v-3)+9r(v-1)]}{9n(v-1)^3} \quad (26)$$

P_1 can be obtained from

$$\frac{P_1}{nkT}=\frac{A_1}{NkT}+\frac{n^2}{2kT}\sum_{\gamma,\lambda}x_\gamma x_\lambda q_{\gamma\lambda}\epsilon_{\gamma\lambda}\left\{(\alpha_{\gamma\lambda}-p_{\gamma\lambda})\Delta_{\gamma\lambda}^{(v)}(\Delta_{\gamma\lambda}^{-10}-2\Delta_{\gamma\lambda}^{-4})+\alpha_{\gamma\lambda}^{(v)}\left(\frac{2\Delta_{\gamma\lambda}^{-3}}{3}-\frac{\Delta_{\gamma\lambda}^{-9}}{9}\right)+(\beta_{\gamma\lambda}-n_{\gamma\lambda})\Delta_{\gamma\lambda}^{(v)}(\Delta_{\gamma\lambda}^{-11}-2\Delta_{\gamma\lambda}^{-5})+\beta_{\gamma\lambda}^{(v)}\left(\frac{\Delta_{\gamma\lambda}^{-4}}{2}-\frac{\Delta_{\gamma\lambda}^{-10}}{10}\right)+(\omega_{\gamma\lambda}-m_{\gamma\lambda})\Delta_{\gamma\lambda}^{(v)}(\Delta_{\gamma\lambda}^{-12}-2\Delta_{\gamma\lambda}^{-6})+\omega_{\gamma\lambda}^{(v)}\left(\frac{2\Delta_{\gamma\lambda}^{-5}}{5}-\frac{\Delta_{\gamma\lambda}^{-11}}{11}\right)+\frac{\alpha_{\gamma\lambda}^{(v)}}{3}\left(\delta_{\gamma\lambda}^{3}-\frac{8}{3}\right)+\frac{\beta_{\gamma\lambda}^{(v)}}{2}\left(\delta_{\gamma\lambda}^{2}-\frac{9}{5}\right)+\omega_{\gamma\lambda}^{(v)}\left(\delta_{\gamma\lambda}-\frac{72}{55}\right)-M^{(v)}\right\} \quad (27)$$

The quantities $\alpha_{\gamma\lambda}^{(v)}$, $\beta_{\gamma\lambda}^{(v)}$, $\omega_{\gamma\lambda}^{(v)}$, $\Delta_{\gamma\lambda}^{(v)}$, and $M^{(v)}$ are the derivatives of the corresponding magnitudes with respect to the number density and were not presented previously, but they appear in Appendix A of this work.

To determine vapor–liquid equilibria, the chemical potential is needed. We have presented analytical expressions for the Helmholtz free energy (see eq 23) and for the pressure (see eqs 24–27). The chemical potential can easily be obtained from the relation

$$\frac{\mu}{kT}=\frac{A}{NkT}+\frac{P}{nkT} \quad (28)$$

Finally, we give here the corresponding equation for entropy, namely, the derivative of Helmholtz free energy with respect to the temperature:

$$S=-(\partial A/\partial T)_V \quad (29)$$

The dependence of contact PCF on temperature could only come from the dependence of the thickness of hard convex bodies in eq 13, and the explicit equations are

$$\frac{S}{Nk}=\frac{S_0}{Nk}+\frac{S_1}{Nk} \quad (30)$$

where

$$\frac{S_0}{Nk}=-\frac{A_0^{hcb}-A^*}{NkT}-\frac{(s^2q^{(T)}+2q)v-2qsv^{(T)}}{9nv^3}+\frac{(r^{(T)}s+s^{(T)}r)(v-1)+rsv^{(T)}}{n(1-v)^2}-\frac{v(s^2q^{(T)}+2sqs^{(T)})(v-1)+qs^2v^{(T)}(1-3v)}{9nv^2(1-v)^2} \quad (31)$$

$$\frac{S_1}{Nk}=-\frac{n}{2k}\sum_{\gamma,\lambda}x_\gamma x_\lambda q_{\gamma\lambda}\epsilon_{\gamma\lambda}\left\{(\alpha_{\gamma\lambda}-p_{\gamma\lambda})\Delta_{\gamma\lambda}^{(T)}(\Delta_{\gamma\lambda}^{-10}-2\Delta_{\gamma\lambda}^{-4})+\alpha_{\gamma\lambda}^{(T)}\left(\frac{2\Delta_{\gamma\lambda}^{-3}}{3}-\frac{\Delta_{\gamma\lambda}^{-9}}{9}\right)+(\beta_{\gamma\lambda}-n_{\gamma\lambda})\Delta_{\gamma\lambda}^{(T)}(\Delta_{\gamma\lambda}^{-11}-2\Delta_{\gamma\lambda}^{-5})+(\beta_{\gamma\lambda}^{(T)}-n_{\gamma\lambda}^{(T)})\left(\frac{\Delta_{\gamma\lambda}^{-4}}{2}-\frac{\Delta_{\gamma\lambda}^{-10}}{10}\right)+(\omega_{\gamma\lambda}-m_{\gamma\lambda})\Delta_{\gamma\lambda}^{(T)}(\Delta_{\gamma\lambda}^{-12}-2\Delta_{\gamma\lambda}^{-6})+(\omega_{\gamma\lambda}^{(T)}-m_{\gamma\lambda}^{(T)})\left(\frac{2\Delta_{\gamma\lambda}^{-5}}{5}-\frac{\Delta_{\gamma\lambda}^{-11}}{11}\right)+\frac{\alpha_{\gamma\lambda}^{(T)}}{3}\left(\delta_{\gamma\lambda}^{3}-\frac{8}{3}\right)+\alpha_{\gamma\lambda}\delta_{\gamma\lambda}^{2}\delta_{\gamma\lambda}^{(T)}+\frac{\beta_{\gamma\lambda}^{(T)}}{2}\left(\delta_{\gamma\lambda}^{2}-\frac{9}{5}\right)+\alpha_{\gamma\lambda}\delta_{\gamma\lambda}\delta_{\gamma\lambda}^{(T)}+\omega_{\gamma\lambda}^{(T)}\left(\delta_{\gamma\lambda}-\frac{72}{55}\right)+\omega_{\gamma\lambda}\delta_{\gamma\lambda}^{(T)}-M^{(T)}\right\} \quad (32)$$

As above, subscripts 0 refers to reference contribution and 1 to perturbation contribution. Superscript (T) of the variables in eqs 31 and 32 refers to derivatives with respect to the temperature, and the explicit expressions are given elsewhere.[17] Since these derivatives are not necessary to compute VLE, they are not used in this paper.

Equations 23–32 look complicated, but their terms are analytic and, therefore, quite convenient to compute. Moreover they are related to the molecular energy, size, and shape. Therefore the presented equations as well as any further improvement or correction to these equations have a clear physical meaning.

III. Comparison with Simulation

As previously pointed out, simulation for linear molecules interacting with Kihara potentials have been performed in the Gibbs ensemble.[9] These simulations provide exact results for coexistence properties of molecular models. We obtained unambiguous result regarding the validity range of our theory by applying it to these models. Figures 1 and 2 show results obtained

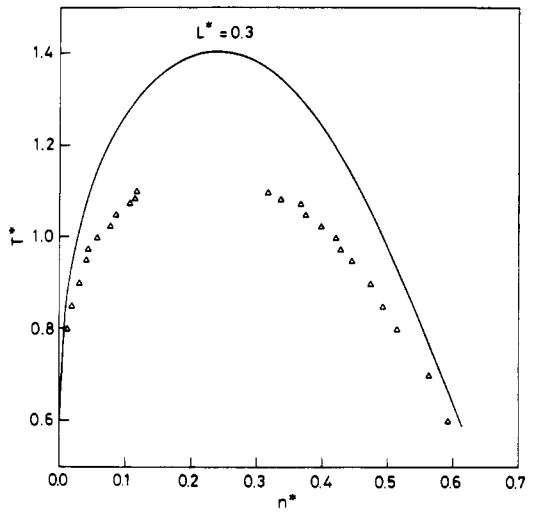

Figure 1. Vapor–liquid equilibrium for a linear Kihara model with $L^* = 0.3$. The reduced temperature T^* and density n^* are defined as $T^* = T/(\epsilon/k)$ and $n^* = n\sigma^3$. The solid line corresponds to the results of this work (SPT) and symbols to simulations of ref 9.

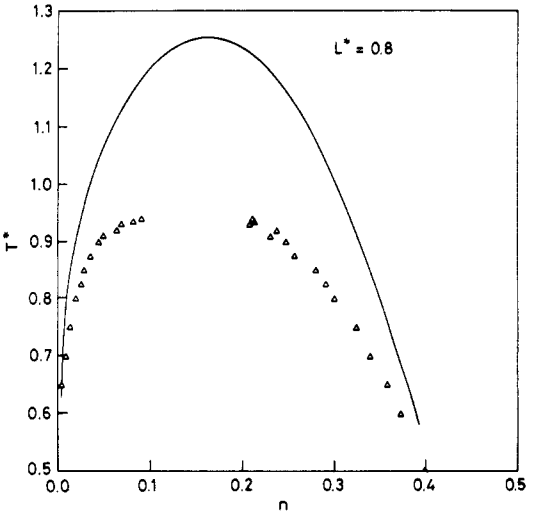

Figure 2. As in Figure 1 with $L^* = 0.8$.

from the theory and from Monte Carlo simulations for two different elongations, roughly corresponding to nitrogen and carbon dioxide. In both cases there is good agreement between theory and simulation from approximately the triple point up to $T^* \simeq 0.8T^*_c$. These figures also show that theory always overestimates the coexistence density on the liquid branch and underestimates it on the vapor branch. At higher temperatures theoretical results deviate significantly from simulation, and SPT predicts excessively high critical temperatures. The rigorous perturbation theory RPT yields much better agreement when compared with computer simulation results as shown in a previous work.[9] However, RPT is quite involved and probably not useful for practical applications in its present form.

The SPT of this work may be useful for practical applications even if as illustrated in Figures 1 and 2 not quite satisfactory agreement with simulation is obtained at high temperatures. When semiempirical EOS is used, some parameters are usually chosen to fit experimental properties. We also can follow this method. If the solid line of Figure 1 is moved downward so that the critical point of theory is forced to match the simulation value, better agreement between theory and simulation for VLE is obtained. Of course, this method is not allowed from a purely theoretical point of view. However, this is done when any theoretical value is forced to match an experimental point. The SPT may be quite useful if some potential parameters are obtained by fitting them to a few experimental results. In the next section it is shown that

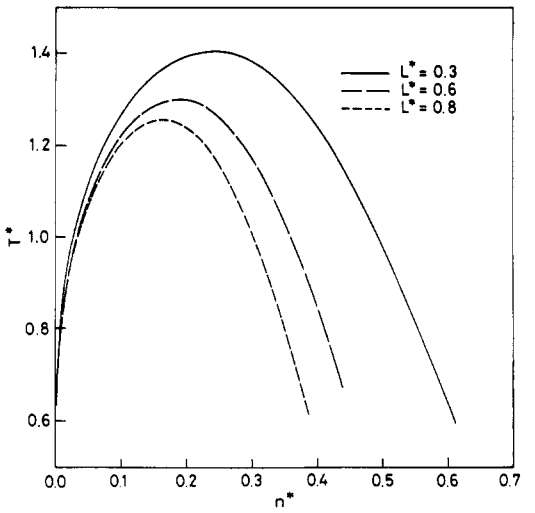

Figure 3. Variation of vapor–liquid equilibrium curve with molecular elongation for linear Kihara models as obtained from the SPT of this work. Units as in Figure 1.

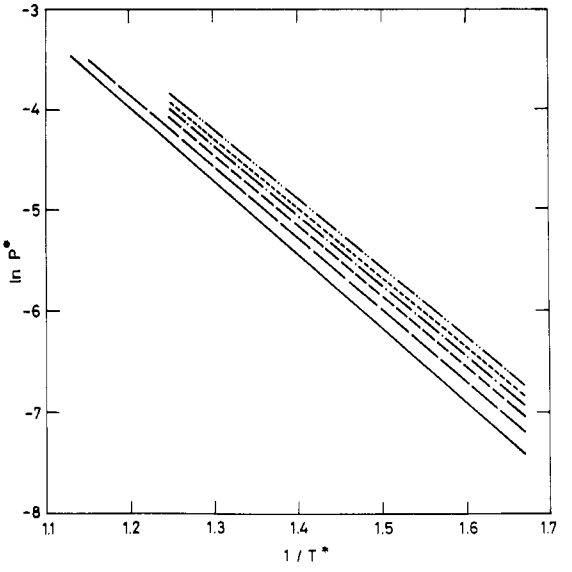

Figure 4. Logarithm of vapor pressure versus temperature inverse for linear Kihara models with different elongations. From top to bottom these elongations are $L^* = 1.0$, 0.6, 0.5, 0.4, 0.3, and 0.2.

good agreement with experiment is still possible if a fitting to a few experimental data is performed.

To illustrate the trends with elongation of VLE, Figure 3 presents the VLE for three elongations as obtained from SPT. Figure 3 shows that the VLE curve, as obtained from the theory, becomes narrower (in the used units) when the molecular elongation increases. Therefore a best empirical fitting to simulation can occur if a greater elongation is used for the theoretical model than for the simulated one. The practical consequences of this are described in section IV.

Vapor enthalpy is also an important property of liquids. Clausius–Clapeyron classical law predicts a linear variation of vapor pressure with temperature inverse.[18] Figure 4 shows that this prediction is fulfilled by the theory presented here, and a similar behavior has been reported for simulation.[9] However, reduced vapor enthalpy, defined as

$$\Delta H_v = \mathrm{d} \ln p^* / \mathrm{d}(1/T^*) \tag{33}$$

namely, the slope of the represented straight line, is greater for the theory the difference being about 15% above simulation results.

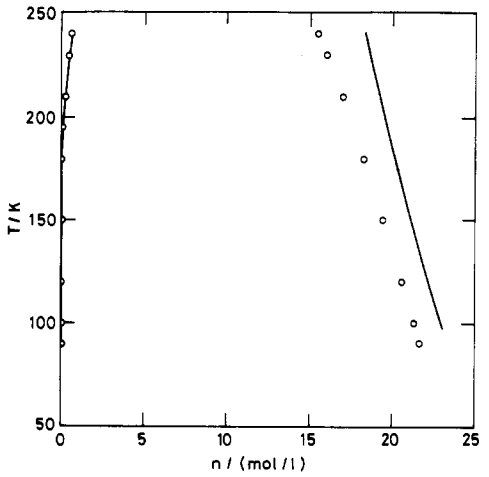

Figure 5. Vapor–liquid equilibrium curve for ethane with $L^* = 0.5$. Circles are experimental points from ref 20 and solid line the theory presented in this work with the parameters of Table 1.

TABLE 1: Intermolecular Potential Parameters of Substances Considered in This Work

substance	ϵ/k (K)	σ (Å)	L^*
ethane	317.37	3.466	0.5
ethane	317.37	3.466	0.6
carbon dioxide	338.01	2.902	0.8
benzene	782.97	2.834	0.68

IV. Comparison with Real Substances

The following step, the most important from an industrial point of view, is comparison of theoretical results with experiment. Presented here are the results for the linear molecules, ethane, and carbon dioxide and for the nonlinear molecule benzene. Benzene is modeled as a set of bonds preserving the molecular shape and eq 1 applies to the closest distance between the bonds of two molecules.

Intermolecular parameters for ethane were taken from ref 19. These parameters were obtained by using RPT and are shown in Table 1. It was necessary to check if potential parameters obtained from the rigorous version of the perturbation theory could still be useful in the context of the simple version of this work (SPT). In Figure 5 the VLE for ethane as obtained from experiment and from the SPT of this work is presented. The agreement is not quite satisfactory. Theory always overestimated liquid density and underestimated vapor density, showing systematic differences similar to those reported above in comparison with simulations. Thus, it appears that a more elongated model could agree better with experimental results. This observation is correct. We repeated the computations for a model of ethane with the same parameters ϵ and σ given in Table 1 but with $L^* = 0.6$, and the agreement was excellent as shown in Figure 6. In fact, it was better than 2% over a temperature range of more than 100 K. Ethane is a relatively simple molecule, but it is extremely important in the natural gas industry.

We conclude that the set of parameters previously proposed by us[6] for a number of real substances with the RPT may still be used with the computationally more convenient SPT by slightly changing the molecular elongation L^* thus providing a route for practical applications.

However, another route may be useful. In fact, ϵ/k and σ can be determined for a given substance by forcing the SPT predictions to match some experimental properties. A simple and fast procedure is to match the experimental vapor pressure and orthobaric density at a given temperature. Therefore, only one point of the coexistence curve is needed. This is by far less demanding than the number of experimental data required by semiempirical EOS to determine their parameters. We determined by this procedure ϵ/k and σ for carbon dioxide and benzene.

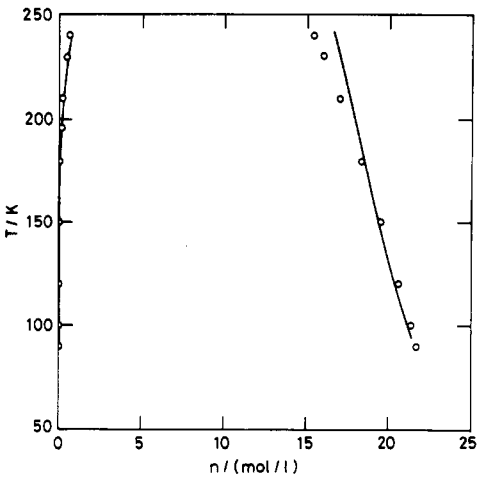

Figure 6. As in Figure 5 but for a model with $L^* = 0.6$.

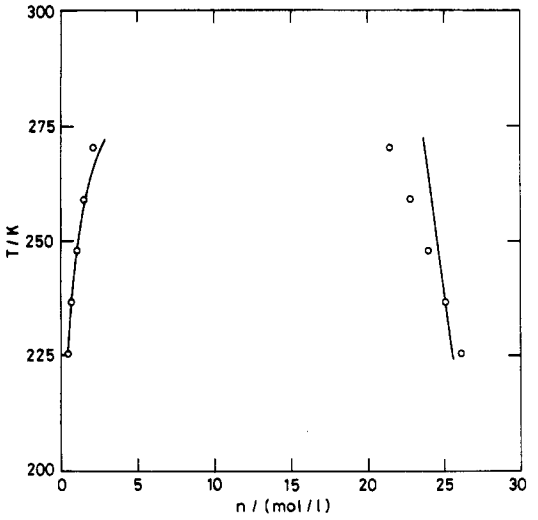

Figure 7. As in Figure 5 but for carbon dioxide. Experimental points from ref 21. Potential parameters are given in Table 1.

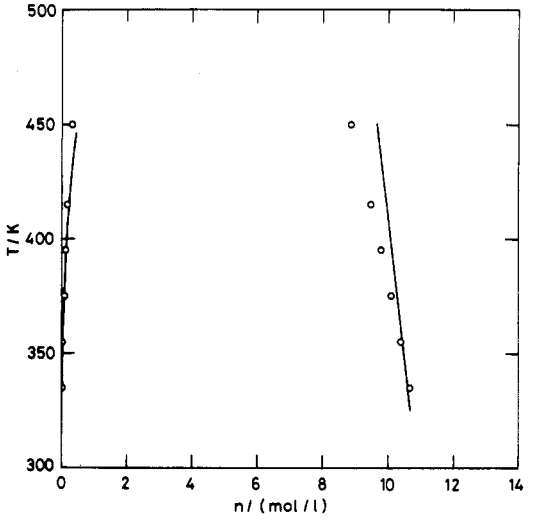

Figure 8. As in Figure 5 but for benzene. Experimental points from ref 22. Potential parameters are given in Table 1.

The parameters obtained in this way are shown in Table 1. In Figures 7 and 8 are shown the obtained VLE densities for carbon dioxide and benzene. The agreement between theory and experiment is good. It should be recognized, however, that in the case of CO_2 the quadrupole moment plays an important role in its thermodynamic properties, and a nonpolar model may prove to be insufficient to describe it. More elaborated calculations for CO_2 should include this quadrupolar contribution. This sug-

TABLE 2: Orthorbaric Densities n_l (mol/L), Vapor Pressures P (MPa), and Vapor Densities n_g (mol/L) As Obtained from Experiment and from the SPT Theory of This Work with the Parameters of Table 1[a]

T/K	n_l^{exp}	n_l^{SPT}	n_g^{exp}	n_g^{SPT}	P^{exp}	P^{SPT}
			Ethane			
100.00	21.34	21.10	1.7×10^{-6}	2.2×10^{-5}	1.1×10^{-5}	1.7×10^{-6}
120.00	20.60	20.35	8.6×10^{-5}	1.0×10^{-4}	3.5×10^{-4}	1.0×10^{-4}
150.00	19.47	19.37	3.5×10^{-3}	4.2×10^{-3}	9.7×10^{-3}	5.0×10^{-3}
180.00	18.28	18.46	3.6×10^{-2}	4.2×10^{-2}	7.9×10^{-2}	6.0×10^{-2}
210.00	16.97	17.60	0.187	0.203	0.334	0.335
230.00	16.04	17.03	0.452	0.487	0.700	0.824
240.00	15.46	16.76	0.679	0.739	0.967	1.232
			Carbon Dioxide			
225.34	26.08	25.53	0.42	0.41	0.75	0.71
236.61	25.06	25.06	0.65	0.69	1.15	1.15
247.87	23.96	24.58	1.03	1.02	1.67	1.79
259.14	22.77	24.18	1.47	1.60	2.35	2.73
270.41	21.42	23.7	2.07	2.66	3.23	4.08
			Benzene			
445.78	8.94	9.69			0.90	1.49
413.40	9.50	9.96			0.47	0.68
381.24	10.00	10.23			0.22	0.27
362.84	10.28	10.39			0.13	0.15
344.49	10.54	10.54			7.7×10^{-2}	7.7×10^{-2}
326.12	10.80	10.70			4.1×10^{-2}	3.6×10^{-2}

[a] We present results for ethane, carbon dioxide and benzene. In the case of ethane we used $L^* = 0.60$. Experimental data of ethane, carbon dioxide and benzene were taken from Refs [20,21,22] respectively.

gestion illustrates the point that molecular-based theories are easier to improve since discrepancies have a clear molecular origin.

To provide further comparison between the results of the SPT and experimental data, coexistence properties are presented in Table 2 for ethane, carbon dioxide, and benzene. It can be seen that SPT provides reasonable predictions of coexistence properties.

The results shown in this section are simpler and more accurate than those arising from the most widely used empirical EOS. Furthermore, they are molecular based so that a pictorial insight can be obtained directly from our computations.

V. Conclusions

As previously mentioned, a second important parameter for liquids is the vapor enthalpy, ΔH_v. The agreement between theory and experiment is not so good in this case, but it remains acceptable. Figure 4 shows that the reduced vapor enthalpy is nearly independent of temperature on a broad range, but it varies smoothly with molecular elongation. Moreover, the calculated vapor enthalpy is for ethane $\Delta H_v = 19.2$ kJ/mol for the model with $L^* = 0.6$ overestimating the experimental value[20] of $\Delta H_v \cong 17.7$ kJ/mol for the temperatures considered in this work. Furthermore, RPT has a similar absolute error but underestimates the value[19] of ΔH_v as 14.9 kJ/mol.

A second noteworthy feature of the theory presented here is the feasibility of applying it to mixtures. For the sake of clarity and taking into account that simulations for mixtures of Kihara molecules are not available, results for mixtures are not discussed here, but our FORTRAN program is indeed written for a multicomponent system and is available upon request.

The theory proposed in this work based on statistical mechanics, with the help of a bit of empirical character based always in comparison with simulation and using magnitudes with physical meaning, is quite simple to implement. Because of that it may be of interest to the chemical industry and to those engaged in pure research.

Acknowledgment. This work has been financially supported by Project PB91-0364 of the Spanish DGICYT (Direccion General de Investigación Científica y Técnica). B.G. would like to thank Universidad Complutense the award of a predoctoral grant. We would like to thank Erik Luddin for improving the English of our first version.

Appendix A

Symbols appearing in eq 23 are related to molecular geometry as follows:

$$m_{\gamma\lambda} = S_{\gamma\lambda} + 4\pi d_{\gamma\lambda} - 8\pi R_{\gamma\lambda} d_{\gamma\lambda} \tag{A1}$$

$$n_{\gamma\lambda} = 8\pi R_{\gamma\lambda} q_{\gamma\lambda} - 8\pi q_{\gamma\lambda} d_{\gamma\lambda} \tag{A2}$$

$$p_{\gamma\lambda} = 4\pi q_{\gamma\lambda}^2 \tag{A3}$$

$$t_{\gamma\lambda} = S_{\gamma\lambda} - 4\pi R_{\gamma\lambda} d_{\gamma\lambda} \tag{A4}$$

$$\nu_{\gamma\lambda} = 4\pi R_{\gamma\lambda} q_{\gamma\lambda} \tag{A5}$$

$$\alpha_{\gamma\lambda} = (A_{\gamma\lambda} + 1) p_{\gamma\lambda} \tag{A6}$$

$$\beta_{\gamma\lambda} = n_{\gamma\lambda}(A_{\gamma\lambda} + 1) + \nu_{\gamma\lambda}(g_{\gamma\lambda}^{hcb}(0) - 1 - A_{\gamma\lambda}) \tag{A7}$$

$$\omega_{\gamma\lambda} = m_{\gamma\lambda}(A_{\gamma\lambda} + 1) + t_{\gamma\lambda}(g_{\gamma\lambda}^{hcb}(0) - 1 - A_{\gamma\lambda}) \tag{A8}$$

$$M = n x_\gamma x_\lambda g_{\gamma\lambda}^{hcb}(0) S_{\gamma+d+\lambda} \{ d_{\gamma\lambda} - \int_0^{q_{\gamma\lambda}} (1 - \exp[-\beta u_0^{\gamma\lambda}])\, d\rho \} \tag{A9}$$

The integral appearing in M has been parameterized by Verlet and Weis[23] and can be computed as

$$H \equiv \int_0^{q_{\gamma\lambda}} (1 - \exp[-\beta u_0^{\gamma\lambda}])\, d\rho = \sigma_{\gamma\lambda}(0.3837 + 1.068 T^{*-1})/(0.4293 + T^{*-1}) \tag{A10}$$

The derivatives appearing in eq 27 of the main text are given by

$$\alpha^{(v)} = (\partial \alpha_{\gamma\lambda}/\partial n) = p_{\gamma\lambda} A_{\gamma\lambda}^{(v)} \tag{A11}$$

$$\beta_{\gamma\lambda}^{(v)} = (\partial \beta_{\gamma\lambda}/\partial n) = n_{\gamma\lambda} A_{\gamma\lambda}^{(v)} + \nu_{\gamma\lambda}(g_{\gamma\lambda}^{(v)}(0) - A_{\gamma\lambda}^{(v)}) \tag{A12}$$

$$\omega_{\gamma\lambda}^{(v)} = (\partial \omega_{\gamma\lambda}/\partial n) = m_{\gamma\lambda} A_{\gamma\lambda}^{(v)} + t_{\gamma\lambda}(g_{\gamma\lambda}^{(v)}(0) - A_{\gamma\lambda}^{(v)}) \tag{A13}$$

$$M^{(v)} = \left(\frac{\partial M}{\partial n}\right) = M\left(\frac{1}{n} + \frac{g_{\gamma\lambda}^{(v)}(0)}{g_{\gamma\lambda}^{hcb}(0)}\right) \tag{A14}$$

$$\Delta_{\gamma\lambda}^{(v)} = (\partial \Delta_{\gamma\lambda}/\partial n) = b_{\gamma\lambda}^{(v)}/q_{\gamma\lambda} \tag{A15}$$

These functions themselves depend on $g_{\gamma\lambda}^{(v)}(0)$, $b_{\gamma\lambda}^{(v)}$, $A_{\gamma\lambda}^{(v)}$ whose explit expressions are

$$g_{\gamma\lambda}^{(v)}(0) = \frac{1}{n(v-1)^2} + \frac{S_\gamma S_\lambda (r-t) + (S_\gamma T_\lambda - T_\gamma S_\lambda) s}{n(1-v)^3 S_{\gamma+\lambda}}(v+1) + \frac{2 S_\gamma S_\lambda q s (v+2)}{9n(1-v)^4 S_{\gamma+\lambda}} = \left(\frac{\partial g_{\gamma\lambda}^{hcb}(0)}{\partial n}\right) \tag{A16}$$

$$b_{\gamma\lambda}^{(v)} = -(g_{\gamma\lambda}^{(v)}(0) R_{\gamma\lambda}/[g_{\gamma\lambda}^{hcb}(0)]^2) \tag{A17}$$

$$A_{\gamma\lambda}^{(v)} = -\frac{(2\pi R_{\gamma\lambda}^2 + g_{\gamma\lambda}^{hcb}(0) S_{\gamma\lambda})([g_{\gamma\lambda}^{hcb}(0)]^2 + 2 g_{\gamma\lambda}^{hcb}(0) - 1)}{2\pi R_{\gamma\lambda}^2 (g_{\gamma\lambda}^{hcb}(0) + 1)^2} \tag{A18}$$

References and Notes

(1) Reid, R. C.; Prausnitz, J. M.; Poling, B. E. *The Properties of Gases and Liquids*, 4th ed.; McGraw-Hill: New York, 1987.
(2) Redlich, O.; Kwong, J. N. S. *Chem. Rev.* **1949**, *44*, 233.
(3) Peng, D. Y.; Robinson, D. B. *Ind. Chem. Eng. Fund.* **1976**, *15*, 59.
(4) Deiters, V. *Chem. Eng. Sci.* **1981**, *36*, 1139.
(5) Saez, C.; Compostizo, A.; Rubio, R. G.; Crespo Colín, A.; Diaz Peña, M. *J. Chem. Soc., Faraday Trans.* **1986**, *82*, 1839.
(6) Vega, C.; Lago, S.; Padilla, P. *J. Phys. Chem.* **1992**, *96*, 1900.
(7) Lago, S.; Boublík, T. *Coll. Czech. Chem. Commun.* **1980**, *45*, 3051.
(8) Kihara, T. *J. Phys. Soc. Jpn.* **1951**, *16*, 289.
(9) Vega, C.; Lago, S.; De Miguel, E.; Rull, L. F. *J. Phys. Chem.* **1992**, *96*, 7431.
(10) Lado, F. *Phys. Rev.* **1973**, *A8*, 2548.
(11) Vega, C.; Lago, S. *Mol. Phys.* **1991**, *72*, 215.
(12) Vega, C.; Lago, S. *Chem. Phys. Lett.* **1991**, *185*, 516.
(13) Vega, C.; Lago, S. *J. Chem. Phys.* **1990**, *93*, 8171.
(14) Hadwiger, H. *Altes und neues über konvexe Körper*; Birkäuser: Basel, 1955.
(15) Weeks, J. D.; Chandler, D.; Andersen, H. C. *J. Chem. Phys.* **1971**, *54*, 5237.
(16) Barker, J. A.; Henderson, D. *J. Chem. Phys.* **1967**, *47*, 4714.
(17) López-Martin, J. L. Master Thesis, Universidad Complutense, Madrid, 1993.
(18) Klotz, I. M.; Rosenberg, R. M. *Chemical Thermodynamics*; 3rd ed.; Benjamin: Menlo Park, CA, 1972.
(19) Vega, C. *Termodinàmica Estadística del Estado Líquido*; Complutense: Madrid, 1991.
(20) Younglove, B. A.; Ely, J. F. *J. Phys. Chem. Ref. Data* **1987**, *16*, 577.
(21) Angus, S.; Armstrong, B.; De Reuck, K. S. *International Thermodynamic Tables of Fluid State*; Pergamon Press: New York, 1973; Vol. 3, *Carbon Dioxide*.
(22) Kratzke, H.; Niepmann, R.; Spillner, E.; Kohler, F. *Fluid Phase Equil.* **1984**, *16*, 287.
(23) Verlet, L.; Weis, J. J. *Phys. Rev.* **1972**, *A5*, 939.